SRF EXPERIENCE WITH THE CORNELL HIGH-CURRENT ERL INJECTOR PROTOTYPE*

M. Liepe†, S. Belomestnykh, E. Chojnacki, Z. Conway, V. Medjidzade, H. Padamsee, P. Quigley, J. Sears, V. Shemelin, V. Veshcherevich, CLASSE, Cornell University, Ithaca NY, USA

Abstract

Cornell University has developed and fabricated a SRF injector cryomodule for the acceleration of the high current (100 mA) beam in the Cornell ERL injector prototype. The injector cryomodule is based on superconducting rf technology with five 2-cell rf cavities operated in the cw mode. To support the acceleration of a low energy, ultra low emittance, high current beam, the beam tubes on one side of the cavities have been enlarged to propagate Higher-Order-Mode power from the cavities to broadband RF absorbers located at 80 K between the cavities. The axial symmetry of these absorbers, together with two symmetrically placed input couplers per cavity, avoids transverse on-axis fields, which would cause emittance growth. Each cavity is surrounded by a LHe vessel and equipped with a frequency tuner including fast piezo-driven fine tuners for fast frequency control. The cryomodule provides the support and precise alignment for the cavity string, the 80 K cooling of the HOM loads, and the 2 K LHe cryogenic system for the high cw heat load of the cavities. In this paper results of the commissioning phase of this cryomodule will be reported.

MOTIVATION

Cornell University's Laboratory for Accelerator based Sciences and Education is currently exploring the potential of a x-ray light source based on the Energy-Recovery-Linac (ERL) principle [1], which promises superior X-ray performance as compared to conventional third generation light sources [2]. As a first step, to study and demonstrate the production and preservation of a high current, ultra-low emittance beam, a prototype of the ERL injector has been developed and constructed, see Figure 1. This injector is currently under commissioning [3]. One of the most challenging and critical components in the injector is its superconducting radio-frequency (SRF) cryomodule, hosting five SRF 2-cell 1.3 GHz cavities. The cavities in the module are powered by individual high power (120 kW) CW klystrons, located on a mezzanine above the injector prototype. All infrastructure required to operate this cryomodule is in place, including the cryogenic refrigerator, high power klystrons, and a digital LLRF control system, see Fig. 2. In the following we first give a short summary of the module design and assembly and then report in more detail on first results from the ongoing commissioning and performance testing of this injector module and its infrastructure.

* Work supported by NSF Grant No. PHY-0131508 and NSF/NIH-NIGMS Grant No. DMR-0225180.

† MUL2@cornell.edu

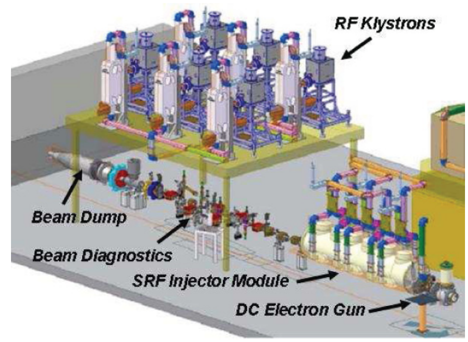

Figure 1: Layout of the ERL injector prototype.

Figure 2: Left: 120 kW CW klystrons. Right, top: Cryogenic pumps. Right, bottom: LLRF control hardware.

MODULE DESIGN AND INNOVATIONS

The ERL injector cryomodule design is based on the TTF cryomodule [4], with beam line components supported from a large diameter helium gas return pipe (HGRP) and all cryogenic piping located inside the module. This concept has been significantly redesigned to fulfill ERL specific requirements, which include (1) the acceleration of a high current beam with up to 500 kW of total power transferred to the beam, (2) significant Higher-Order Mode (HOM) power extraction from the SRF cavities, (3) the preservation of the ultra-low emittance of the electron beam, and (4) CW cavity operation with high cryogenic loads. Table 1 lists some of the key specifications of the injector cryomodule. This module also serves as a conceptual prototype for ERL main linac [5]. Key features and innovations of the injector prototype cryomodule include among others (see also Fig. 3 and Table 1): (1) A symmetric beamline avoids transverse on-axis fields, which would cause emittance growth. (2) The 2K, 4.5K, and 80K cryogenic systems in the module have been upgraded to intercept the

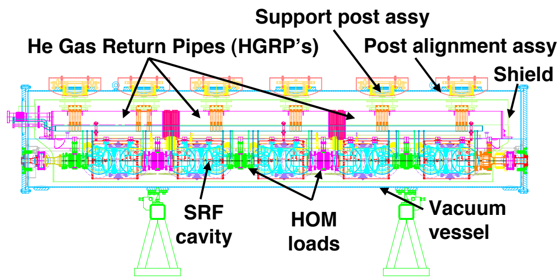

Figure 3: Longitudinal cross-section of the ERL injector module with 5 SRF cavities with HOM beam line absorbers in between. The module is longitudinally separated in three sections, each supported and aligned independently.

Table 1: ERL injector cryomodule specifications.

Numb. of cavities / HOM loads	5 / 6
Accelerating voltage per cavity	1 - 3 MV
Fundamental mode frequency	1.3 GHz
R/Q (circuit definition) per cavity	111 Ohm
Loaded quality factor	4.6×10^4 to 10^6
RF power installed per cavity	120 kW
Required amplit. / phase stab. (rms)	1×10^{-3} / $0.1°$
Maximum beam current (design)	100 mA
Total 2K / 5K / 80K loads	$\approx$ 26 / 60 / 700 W
Overall length	5.0 m

high dynamic heat loads. (3) Three magnetic shield layers effectively shield external magnetic fields. (4) Only one layer of thermal shield (at 80K) is used. (5) Short module end sections minimize the distance between the photo-emission DC gun and the first cavity. (6) Gate-valves on each module end, located inside of the module with their drive units outside of the module, make external gate vales obsolete. (7) A new cavity string alignment concept simplifies module assembly and provides improved alignment tolerances. In this concept, the cavities and HOM loads are supported via precisely machined, fixed supports to the HGRP sections. The alignment of the cavities can be improved even further by adjusting the cavity positions via alignment bolts at the HGRP support posts once the cryomodule is cold. Refer to [6] for details.

MODULE ASSEMBLY

Prototypes of the main beam line components (cavities, HOM loads, input couplers) have been developed, fabricated and tested individually [7, 8, 9]. Following the successful full system test of a one cavity horizontal test cryomodule [10], the full ERL injector SRF cryomodule has been fabricated and assembled; refer to [11] for details. In May 2008, the injector module was installed in the ERL injector, cooled down to 2K, and commissioning has started.

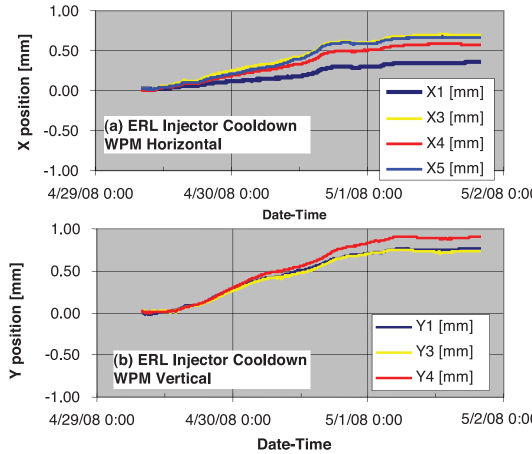

Figure 4: WPM data during cool-down of the injector module. Top: Horizontal position of WPM blocks on cavities 1, 3, 4, and 5. Bottom: Vertical position of WPM blocks on cavities 1, 3, and 4. WPM #2 is not functional.

COOL DOWN AND ALIGNMENT

The cryomodule was cooled down from room temperature to 4.2 K over a period of 2.5 days. Above 80K, the cool-down rate was limited to $<$ 10K/hour to reduce thermal stress. No problems or leaks were found during module cool-down. Fundamental mode frequencies of all cavities were measured after cool-down. Prior to any cavity tuning, a frequency spread of only 17 kHz was found. During cool-down, the shift in cavity positions was monitored by a wire-position-monitor (WPM) system. To each cavity, a WPM block is directly mounted for measuring the horizontal and vertical positions of the cavities independently, see Figure 4. The observed position shifts during cool-down are in very good agreement (within 0.2 mm) with values expected from thermal shrinkage of the cavity support structure and of the WPM block support. After cool down, the maximum transverse alignment errors of the SRF cavities in the injector module are ± 0.2 mm. Such excellent cavity string alignment is important for emittance preservation of the low energy beam in the ERL injector.

STATIC HEAT LOAD

The static heat leak to 1.8K was measured by closing the JT valve in the LHe feed and measuring the LHe boil-off rate. Heaters on the 1.8K system were used for calibration. These measurements give a static heat leak to 1.8K of 10.3 ± 2 W, in good agreement with the expected static 1.8K load of 9 W. The dominating part of this static heat load comes from thermal conduction from "4.5K intercepts" in the input couplers, support posts and HOM absorbers to the 1.8 K system. Currently, the "4.5K system" of the cryomodule is cooled by high pressure helium gas at an elevated temperature of about 6K, as a result of non-ideal heat exchange in the refrigerator system, which increases the estimated total 1.8K static load from 5 W to 9 W.

RF SYSTEM

The injector cryomodule RF system employs five klystrons, each delivering up to 120 kW of CW RF power to individual cavities via twin input couplers [7, 12]. The 7-cavity K3415LS tube manufactured by e2v has a saturated output power of about 160 kWCW. To provide stable regulation of the cavity field, the klystron must have a non-zero gain and therefore cannot operate in saturation. The klystrons passed the factory acceptance test meeting specifications at 135 kW before shipping. The tubes were installed, tested again at Cornell, and are preforming well. Figure 5 shows typical transfer curves of the e2v klystrons, with efficiencies exceeding 50% above 120 kW output power. The commissioning of the injector RF system is described in detail in [13].

INPUT COUPLER

All high power RF twin-input couplers have so far been processed up to 50 kW under full refection, see Figure 6. All couplers conditioned well, reaching these power levels in pulsed operation within 25 to 75 hours of processing (RF on time). None of the input coupler parts were baked after assembly to the beam line. The warm part of the couplers can be baked in situ via heating elements installed on the couplers in the module, if it should be required to reach power levels above 50 kW.

In a search for residual magnetic fields along the beam axis in the injector module, a low energy beam was passed through the module, and its transverse position measured using beam deflections by RF kick fields excited in the coupler regions of the beam pipe with low RF power, while the cavities where detuned strongly, see Figure 7. Detuning the cavities in these measurements by many bandwidths ensured that the fields inside the cavities are small and the change in beam energy is negligible. The beam trajectory obtained this way shows the presence of residual magnetic fields between cavities 2 and 3, as well as 3 and 4. Additional scans with a DC voltage applied to the inner conductors of the input couplers (up to 1000 V), confirm the presence of quadrupole and sextupole like magnetic fields in these regions, but first estimates show that the impact of these fields on the beam emittance should be negligible.

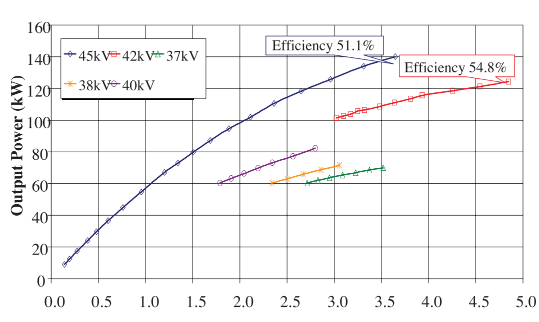

Figure 5: Transfer curve of the ERL injector klystron.

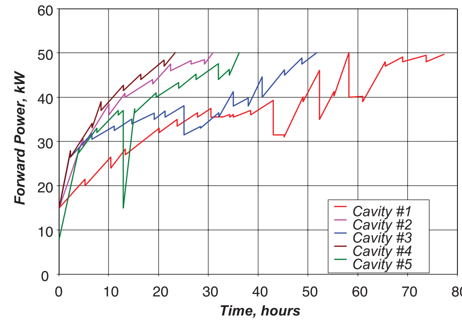

Figure 6: Input coupler processing under full refection (cavity detuned) up to 50 kW. Shown is the maximum forward power per twin-coupler vs. of processing time (pulsed operation with 2 ms pulse length and 20 ms repetition rate).

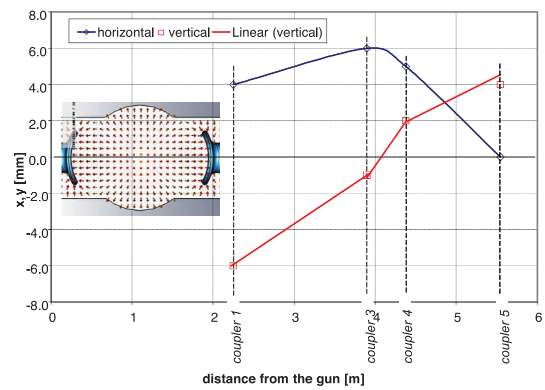

Figure 7: Orbit of a very low energy (250 keV) electron beam in the injector cryomodule as estimated by measuring transverse kicks by the RF fields in the input coupler regions. The RF field is exited by a forward power of up to 1 kW with strongly detuned cavities. The resulting electric RF field has a quadrupole like pattern, as shown on the left. By measuring magnitude and direction of the kick to the beam at a given forward power, the beam position in the coupler region can be determined.

SRF CAVITY PERFORMANCE

All 5 SRF cavities in the injector cryomodule have been performance tested individually at 1.8K to 2K LHe bath temperatures, see Figure 8 and Table 2. In CW mode all cavities reached accelerating voltages of at least 2.8 MV when powered individually (limited by heat flux transfer in the LHe bath), close to the maximum specification of 3 MV. All cavities show field emission at higher fields, and cavity processing is ongoing to further increase maximum field gradients. The cavities also show low intrinsic quality factors below 10^{10} at 2K even at low fields. The exact cause of this is unknown, but first simulations and measurements indicate that losses in the beam tube and coupler regions contribute significantly to the overall dynamic cavity losses. As discussed above, the temperature of the ”4.5K” cooling circuit is elevated at 6K currently, which significantly increases the BCS surface resistance in the cavity end regions, since all cavity flanges are thermally anchored

Table 2: Cavity Performance Summary. (IC: Input coupler vacuum.)

Cavity	CW	Limit	Pulsed	Limit
1	2.8 MV	Cryogenics	4.4 MV	IC
2	3.0 MV	Cryogenics	5.5 MV	IC
3	3.5 MV	Cryogenics	3.7 MV	IC
4	3.4 MV	Cryogenics	4.2 MV	Quench
5	2.8 MV	Quench	5.3 MV	Quench
all	2.4 MV	Cryogenics	-	-

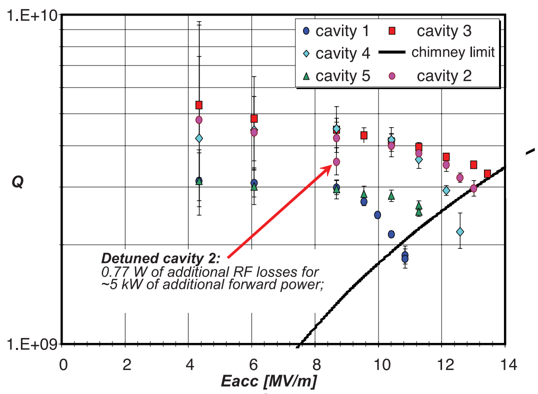

Figure 8: Intrinsic quality factor of the five 2-cell injector SRF cavities as a function of accelerating field gradient at 2K. Also show is the 1 W/cm^2 heat flux limit for the LHe in the chimney connecting the LHe tank around the cavity to the 2K-2 phase LHe supply line.

to that intercept temperature. In addition, early cavity Q measurements shortly after module cool down indicate that the intrinsic quality factors started out around 10^{10}, and might be degrading over time. Note that the cavities on both ends of the module have the lowest Q values.

HOM LOADS

The Higher-Order-Mode absorbers located between the SRF cavities allow for measuring the total HOM power excited by the beam. As of this writing, the maximum beam current passed thought the injector module was 4 mA with 3 pC bunches, exciting only a few mW of HOM power in each cavity, which is too low to be detected. At higher bunch charges and currents, several watts of HOM power will be extracted at each HOM absorber. Heaters mounted on the HOM load bodies are used to calibrate the increase in temperature of the He cooling gas of the loads as a function of power absorbed in each HOM load, see Figure 9.

LLRF FIELD CONTROL

The LLRF electronics for the ERL injector is a new, improved generation of LLRF previously developed for CESR [14], with lower loop latency $< 1\mu$s and increased

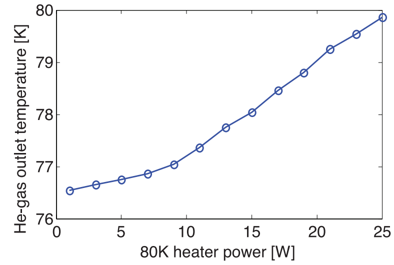

Figure 9: Measured temperature increase of the 80K He outlet gas vs. HOM heater power during calibration.

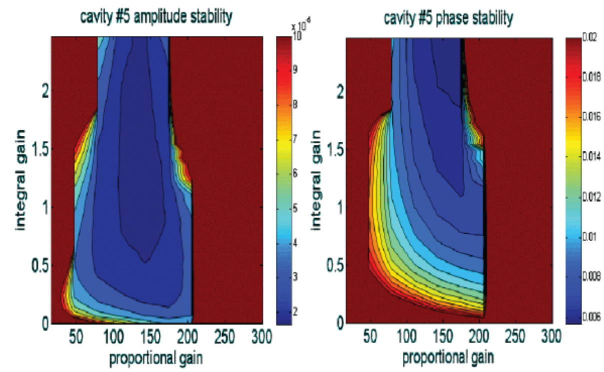

Figure 10: Integral and proportional gain scan to optimize the gains used in the field control loop. Left: Amplitude stability (blue: $\sigma_A/A < 2 \times 10^{-5}$). Right: Phase stability (blue: $\sigma_p < 0.01°$).

sample rates and ADC resolution (16 bits). Integral and proportional gains of the PI loop used to stabilize the RF fields in the SRF cavities have been optimized, as shown in Figure 10 and 11. At optimal gains, exceptional field stabilities of $\sigma_A/A < 2 \times 10^{-5}$ in relative amplitude and $\sigma_p < 0.01°$ in phase (measured against the same reference RF signal used for control) have been achieved, far exceeding the ERL injector and ERL main linac requirements. The main source of field perturbation in the injector cavities is a strong ripple on the high voltage of the klystrons, with relative amplitudes of several percent and frequencies ranging from 360 Hz to may kHz.

CAVITY DETUNING

Though cavity microphonics are not a concern for the ERL injector with its low loaded quality factor cavities, it will be the main field perturbation source in the ERL main lianc, and will determine the RF power required to operate these cavities. Extensive studies on microphonics, its sources and coupling to the SRF cavities, and active detuning compensation have been started therefor on the ERL injector module as a testbed [15, 16]. Typical microphonics levels of a few Hz rms have been found (Figure 12) with significant differences between individual cavities and significant changes over time. Measurements with dynamic sinusoidal forces exerted by a modal shaker on

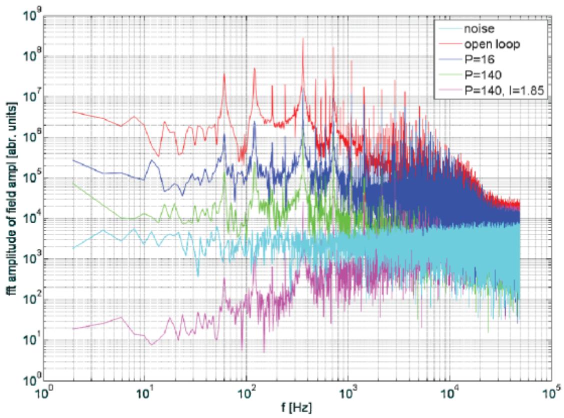

Figure 11: FFT amplitude spectrum of the cavity RF field amplitude for different gain settings. Also shown is the noise spectrum without input connected to the 50 MHz, 16 bit ADC used in sampling the RF field, corresponding to an integrated rms fluctuation of 0.1 bits for f< 50 kHz.

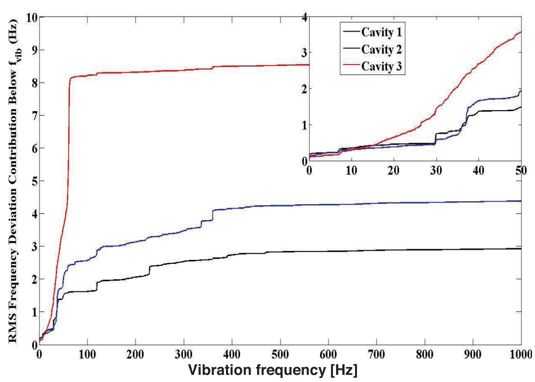

Figure 12: The integrated microphonic spectra for three different cavities in the ERL injector module.

various external parts of the cryomodule (module support, waveguides, beamline, cryolines) show that ground vibrations and other mechanical vibrations do not strongly couple to the SRF cavities, indicating that the major contribution to cavity microphonics comes from fast fluctuations in the sub atmospheric He-pressure and the cryogenic system. Lorentz-force detuning has been compensated reliably using the fast piezoelectric actuators implemented in the cavity frequency tuners in a feedback loop (Figure 13). The motor driven frequency tuner (adapted from the blade tuner design [17]) show good linearity with a frequency resolution of about 2 Hz per step.

OUTLOOK

An extensive commissioning and test program of the SRF ERL injector prototype cryomodule has started, and progresses well. Future work will focus on cavity conditioning, microphonics compensation, and high beam current effects.

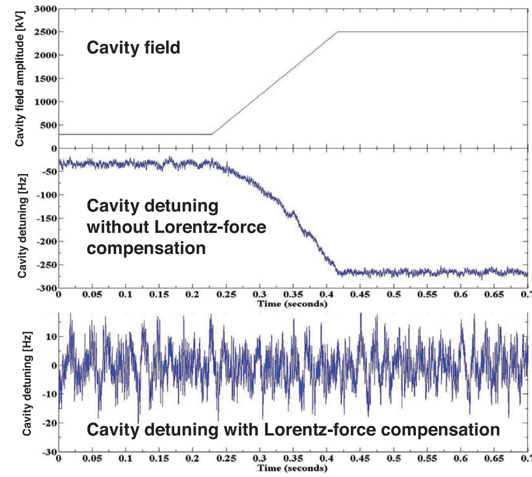

Figure 13: Top: The cavity field is ramped up to 2.5 MV in 0.2 seconds. Middle: Lorentz-force detuning without active compensation. The Lorentz-force detuning coefficient is 2 Hz/(MV/m)^2. Bottom: Cavity detuning during field ramp up with active detuning compensation.

REFERENCES

[1] J. A. Crittenden et al.,"Developments for Cornells...", PAC'09, Vancover, May 2009, paper MO4PBC03 (2009).

[2] D. H. Bilderback, Proceeding of Future Light Sources 2006 meeting in Hamburg, PLT03, p1-6 (2006).

[3] I. Bazarov et al.,"Initial beam results from the Cornell high-current ERL..." PAC'09, Vancover, May 2009 (2009).

[4] C. Pagani et al., Advances in Cryogenic Engineering, Vol. 45A, Edited by Q-S. Shu, Plenum Press, New York (1999).

[5] E. Chojnacki, et al., "Design of an ERL Linac Cryomodule," PAC'09, Vancover, May 2009 (2009).

[6] M. Liepe et al., "Design of the CW Cornell ERL Injector Cryomodule," PAC'05, Knoxvill, TN, USA (2005).

[7] V. Veshcherevich, et al., "Design of High Power Input Coupler...," Proc. of SRF'2005 Workshop (2005).

[8] V. Shemelin, et al., "Dipole-mode-free and kick-free 2-cell Cavity...," Proc. of PAC'03, pp. 2059-2061 (2003).
R. L. Geng, et al., Proc. of PAC'07, pp. 2340-2342 (2007).

[9] V. Shemelin et al., EPAC 2006, Edinburgh, Scotland (2006).
V. Shemelinet al., NIM A 557 (2006) 268-271.

[10] S. Belomestnykh et al., "First Test of the Cornell Single-cavity...," EPAC08, Genoa, Italy, paper MOPP117, (2008).

[11] E. Chojnacki et al., EPAC08, Genoa, Italy, p. 844 (2008).

[12] S. Belomestnykh, et al., "Development of High RF Power Delivery...," LINAC'2004, pp. 694-696 (2004).

[13] S. Belomestnykh et al., "Commissioning of the Cornell ERL...," EPAC08, Genoa, Italy, paper MOPP116, (2008).

[14] M. Liepe et al., PAC'03, Portland, Or, USA (2003).

[15] Z. Conway, M. Liepe, "Electromagnetic and mechanical properties...," PAC'09, Vancover, May 2009 (2009).

[16] Z. Conway, M. Liepe, "Fast piezoelectric actuator control of microphonics...," PAC'09, Vancover, May 2009 (2009).

[17] C. Pagani, "SRF Activities at INFN Milano - Lasa", 10th Workshop of RF Superconductivity, Tsukuba, Japan (2001).